ISSN No:-2456-2165 https://doi.org/10.38124/ijisrt/26nov472

Modeling Earth Returns and Analyzing Faults in SWER System with Heterogeneous Soils

Tsanta Fifaliana Andriamihaja Ramilison[1]; Solofo Hery Rakotoniaina[2]; Harlin Samuel Andriatsihoarana[3]

[1,2,3]Doctoral School of Science and Engineering Techniques and Innovation, University of Antananarivo, Madagascar

Publication Date: 2026/11/18

Abstract: Single wire earth return power lines use the ground as the normal path for return current. Their operating performance and response to faults therefore depend on soil properties. Conventional models generally assume homogeneous soil, although soil resistivity can vary with depth and along the line route. This study proposes an electrical model that accounts for both types of variation. An eighty-kilometer line is divided into ten longitudinal zones, and the Martins Britto formulation is used to represent the layered soil in each zone by an equivalent complex conductivity. The self and mutual impedances are then calculated for each zone. The loop impedance is obtained by subtracting twice the mutual impedance from the sum of the two self-impedances. The Carson formulation serves as the reference, while the Deri approximation supplies the parameters for simulations in Simulink. The model represents the earth return path in heterogeneous soils and supports preliminary engineering and safety assessments. Field measurements are needed to validate the model for a specific site.

Keywords: *Soils Heterogeneity, Soils Stratification, Ground-Return Impedance, Grounding Electrodes.*

How to Cite: Tsanta Fifaliana Andriamihaja Ramilison; Solofo Hery Rakotoniaina; Harlin Samuel Andriatsihoarana (2026) Modeling Earth Returns and Analyzing Faults in SWER System with Heterogeneous Soils. *International Journal of Innovative Science and Research Technology*, 11(11), 582-592. https://doi.org/10.38124/ijisrt/26nov472

I. INTRODUCTION

Single wire earth return (SWER) distribution remains a cost-effective option for sparsely populated areas, as the ground acts as a substitute for the metallic return conductor [1] [2]. However, its simplicity means that a large proportion of the constraints relating to electrical performance – and, above all, safety – are borne by the return path through the ground, as well as by the source and receiver electrodes. Extended supply lines may therefore exhibit a significant voltage drop, an increase in the ground potential of the electrodes (GPR) and contact currents that depend on soil resistivity, electrode geometry and the distance between the source and the contact point [3] [4].

The standard calculations relating to return-to-ground are derived from Carson's integral formulation [5]. Closed-form or logarithmic approximations were subsequently developed to reduce computational effort, notably the complex return-to-ground scheme by Deri et al. [6], Nakagawa's solution for stratified soil [7], Noda's double-logarithmic approximation [8] and Kim's single-logarithmic formulation [9]. Martins-Britto et al. demonstrated that a multi-layer soil profile can be replaced by an equivalent homogeneous conductivity with a small error at the grid frequency [10]. These methods are well established individually, but a real-world SWER feeder may encounter soil heterogeneity in two directions: the vertical sequence of layers determines the local equivalent conductivity, whilst the soil profile also varies longitudinally along the feeder route.

Published SWER studies have focused on voltage maintenance, decentralized generation, conductor sizing, the behavior of communication channels and high-impedance faults [11][12].

The remaining modelling challenge therefore lies in the consistent conversion of heterogeneous ground data into an electrical circuit on a zone-by-zone basis, without double-counting the contribution of the return path to earth. In particular, the term representing the mutual impedance between the overhead conductor and the ground (Zag) in the primitive impedance matrix must remain a coupling term. Representing it as a conductive branch to earth creates an artificial shunt current and consequently invalidates the calculated load and contact currents.

This study aims to develop and numerically verify a model of a SWER feeder line divided into different zones, considering the vertical and longitudinal heterogeneity of the soil. The question that arises is: How can heterogeneous soil

ISSN No:-2456-2165 https://doi.org/10.38124/ijisrt/26nov472

data be consistently converted into zone-specific SWER loop impedances without double-counting the contribution of the return path to earth?

To answer this question, we first homogenize the vertical soil profile in each longitudinal zone. We then derive, for each zone, a primitive impedance matrix, which we convert into the corresponding SWER loop impedance. The source and receiving electrodes are modelled separately from the distributed return impedance via the ground. We then simulate direct and resistive contact between the conductor and earth at various positions along the line. Finally, we verify the model's performance through comparisons with Carson's formulation, analytical circuit solutions and other impedance formulations, as well as by inverting the order of the zones and conducting spatial discretization studies.

The numerical case study used concerns an 80 km SWER power line operating at 12.7 kV, divided into ten longitudinal soil zones and supplying a 100 kVA receiving transformer. This configuration serves as a reproducible reference for evaluating the proposed approach to modelling heterogeneous soils, rather than as a field-validated representation of an existing distribution line. Comparisons in the time domain use a contact point located 44 km from the source, applied at 0.2 s, whilst a separate scan varies its position along the power line. Comparisons with Carson's formulation [5] and analytical circuit calculations [13] confirm the numerical verification. Experimental validation remains necessary, as the soil profiles are simulation scenarios rather than measured route data.

II. METHODE

➢ *Feeder and Soil Representation*

The simulated route is 80.0 km long. This route is divided into ten successive sections, which are 6, 8, 10, 10, 12, 8, 8, 7 and 5 km long respectively as shown in Fig.1. Their boundaries are located at 0, 6, 14, 24, 30, 40, 52, 60, 68, 75 and 80 km. A 22 kV power source supplies a 22/12.7 kV isolation transformer; a 12.7 kV/240 V step-down transformer supplies the declared load of 100 kVA. The conductor resistance used in the model is 5.75 Ω/km, i.e. 460 Ω over 80 km.

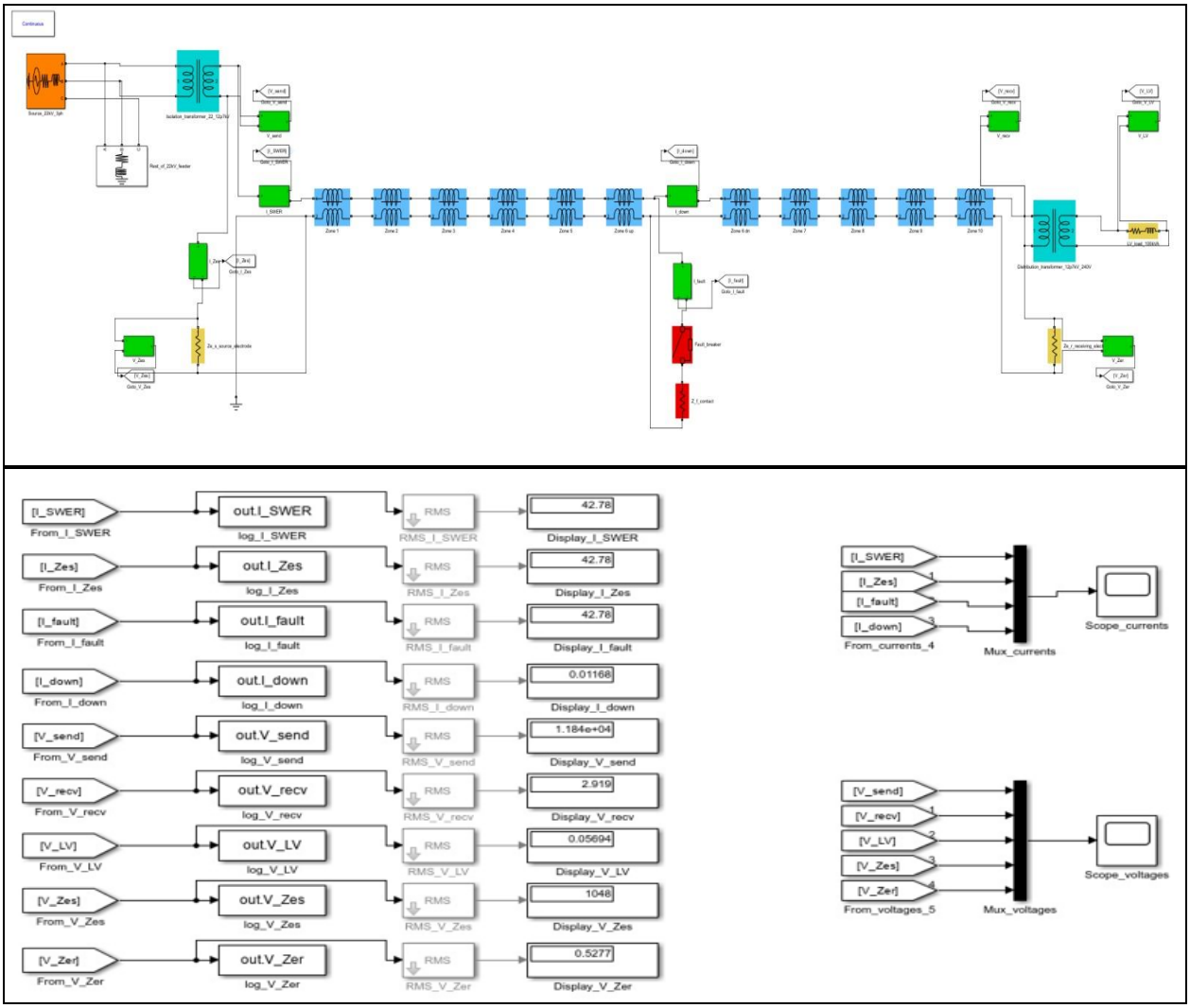


Fig 1 Implementation in MATLAB/Simulink of a Ten-Zone SWER Line, Including the Electrodes, Receiving Transformers, Load and Moving Contact.

ISSN No:-2456-2165 https://doi.org/10.38124/ijisrt/26nov472

For zone k, the vertical soil profile is $S_k = \{(\rho_{k,n}; h_{k,n}), n = 1, \dots, Nk\}$. With $\sigma_{k,n} = \frac{1}{\rho_{k,n}}$, the recursive Martins-Britto operator $H(S_k)$ produces the equivalent complex conductivity σeq_k. The corresponding equivalent resistivity and complex depth are

$$\rho eq_k = \frac{1}{\sigma eq_k} \; ; \quad p_k = \sqrt{\frac{\rho eq_k}{j\omega\mu_0}} \tag{1}$$

The global model therefore retains longitudinal heterogeneity because each zone has its own σeq_k. while the vertical layering within a zone is condensed into a power-frequency equivalent [10].

➢ *Primitive Impedance and SWER Loop*

The SWER system is divided into several longitudinal zones, each comprising the overhead conductor and the underlying ground. Fig 2 illustrates the schematic representation adopted for each zone.

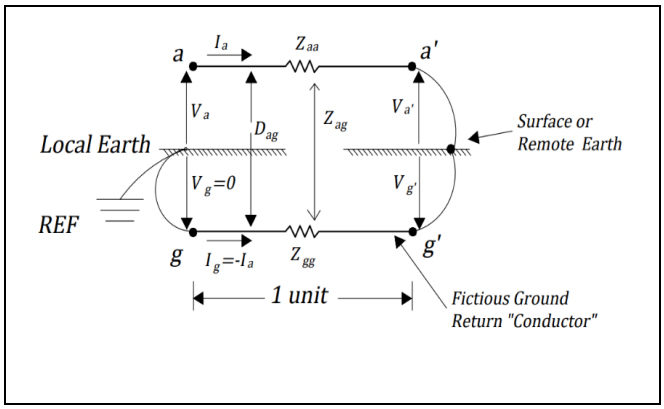


Fig 2 Representation of the Fundamental Impedance of a SWER Line of Unit Length, Showing a Fictitious Return Conductor to Earth.

Each zone is represented by the primitive matrix

$$Z_k = \begin{bmatrix} Zaa_k & Zag_k \\ Zga_k & Zgg_k \end{bmatrix} \tag{2}$$

Where a is the overhead conductor and g is an equivalent earth-return channel. Reciprocity gives $Zag_k = Zga_k$. The same geometric convention, including a 1 m equivalent-channel Geometric Mean Radius (GMR), is applied in every zone [13]:

Using the transformation vector [14]:

$$T_k = \begin{bmatrix} 1 \\ -1 \end{bmatrix} \tag{3}$$

The SWER loop impedance is obtained as:

$$Zloop_k = T_k{}^T Z_k T_k \tag{4}$$

Hence

$$Zloop_k = Zaa_k + Zgg_k - 2Zag_k \tag{5}$$

The zone and feeder impedances are

$$Z_{k\,total} = l_k Zloop_k \tag{6}$$

And

$$Z_{line} = \sum_{k=1}^{N_z} Z_{k\,total} \tag{7}$$

In Simulink, Zaa_k and Zgg_k are assigned to two coupled windings and Zag_k to the mutual coupling. Zag_k is not a physical current path to ground. The separate topology test presented in section 3.6 quantifies the error caused by treating it as a shunt branch.

➢ *Electrodes, Normal Operation, and Fault Equations*

The source and receiver electrodes are represented by concentrated resistances Z_{es} and Z_{er} calculated based on the local soil and a single-rod Dwight approximation [15], in accordance with the earthing practices defined in IEEE Std 80 [16]. These electrode impedances are added together only once; the contribution from the distributed earth return, which is already included in $Zloop$, is not added again. Given the source impedance Z_s, the transformer impedance Z_{tr}, and the SWER-side reference load denoted $Z_{L'}$, the normal current is:

$$I_n = \frac{V_S}{(Z_{es} + Z_{er} + Z_{line} + Z_s + Z_{tr} + Z_{L'})} \tag{8}$$

For a contact at x_f, $Z_{up}(x_f)$ is the sum of the complete upstream zones plus the fraction of the intersected zone. I_f the downstream branch is negligible [13],

$$I_f = \frac{V_S}{(Z_{es} + Z_s + Z_{up}(x_f) + R_f)} \tag{9}$$

When the conductor remains continuous, the contact branch and downstream load branch are retained in parallel. The current source satisfies

$$I_T = I_f + I_{down}. \tag{10}$$

This general representation is required for the 500 Ω contact, because a measurable current continues toward the load.

ISSN No:-2456-2165 https://doi.org/10.38124/ijisrt/26nov472

➢ *Scenarios and Verification Protocol*

Table 1 Definition of the Simulated Scenarios.

Scenario	Soil Configuration	Objective
SC0	Homogeneous soil with a resistivity of 250 Ω.m	Establish the reference response
SC1	Soil varying along the line and with depth	Assess the combined effects of longitudinal and vertical heterogeneity
SC1R	Same soil as SC1, with a contact resistance of 500 Ω	Assess the influence of contact resistance
SC2	Abrupt transition from 50 to 1250 Ω·m	Assess the effect of an abrupt change in soil resistivity
SC3	Reverse zone order of SC2	Assess the influence of zone position
SC4	Progressive variation from 25 to 2500 Ω·m	Assess the effect of a resistivity gradient
SC5	Reverse zone order of SC4	Assess the influence of the gradient direction
SC6	A 200 m thick layer with a resistivity of 80 Ω·m over a 600 Ω·m half-space	Assess the effect of vertical stratification alone

The contact is applied at t=0.2 s in 0.4 s simulations. Verification comprises: (i) Carson, Deri, Noda, Kim, Nakagawa, and study-specific approximation comparisons; (ii) analytical versus simulated normal and fault currents; (iii) a fault-position sweep from the source to 80 km; (iv) reversal of equal sets of zone impedances; (v) 1–40 zone convergence; (vi) soil-resistivity and zone-length sweeps; (vii) a 50 Hz to 10 kHz homogenization test; and (viii) a topology test of Zag

III. RESULTS AND DISCUSSIONS

➢ *Formulation and Circuit Verification*

For SC0 and SC1, the Deri formulation differs from Carson by approximately 0.080–0.081% in mean impedance magnitude and by 0.023–0.024% in calculated fault current. Noda, Kim and Nakagawa also give close results in these comparisons. The approximation proposed in the present study differs from Carson's formulation by approximately 3.10% in mean impedance magnitude and by 0.78–0.87% in fault current. The impedance error is therefore larger than the corresponding current error, because the current also depends on the source, electrode and contact impedances.

For SC0–SC6, excluding SC1R, the simulation-to-analytical difference is approximately 0.297–0.299% for normal current and 0.971–0.998% for fault current. In SC1R, the fault-current difference is approximately 0.727%. This agreement supports circuit implementation but does not constitute experimental validation.

➢ *Scenario Behavior at the 44 km Contact*

The simulated feeder is 80 km long. The contact is located 44 km from the source and is applied at 0.2 s. The contact resistance is 0.01 Ω for all scenarios except SC1R, where it is 500 Ω. Table 2 presents the updated simulation results.

Table 2 Simulation Results for a Contact at 44 km on the 80 km Feeder.

SScenario	Normal current (A)	Contact current (A)	Downstream current (A)	Zes / Zer (Ω)	Source GPR during fault (V)
SSC0	5.774	42.383	0.012	24.51 / 45.18	1039
SSC1	5.726	43.471	0.011	15.99 / 72.29	695
SSC1R	5.726	14.778	3.851	15.99 / 72.29	293
SSC2	5.774	42.465	0.012	24.51 / 45.18	1041
SSC3	5.774	42.300	0.012	24.51 / 45.18	1037
SSC4	5.774	42.454	0.012	24.51 / 45.18	1041
SSC5	5.774	42.311	0.012	24.51 / 45.18	1037
SSC6	5.772	42.318	0.012	24.51 / 45.18	1037

The line impedance magnitude remains between 468.896 and 470.000 Ω. Compared with SC0, SC1 increases line impedance by 0.135% and reduces normal current by 0.827%. The contact current increases from 42.383 to 43.471 A, or 2.57%. SC1 changes both the distributed soil model and the electrode resistances, so this increase cannot be attributed to line heterogeneity alone.

SC1 also changes the earth's potential rise. During normal operation, receiving-electrode GPR increases from 260.44 to 413.25 V. During the fault, source-electrode GPR decreases from 1038.78 to 694.90 V because the source electrode resistance decreases from 24.51 to 15.99 Ω.

In SC1R, the 500 Ω contact reduces contact current to 14.778 A, while 3.851 A still flows towards the load. Source current is 18.354 A. Resistive contact therefore divides current between the contact and the downstream branch, rather than disconnecting the load.

ISSN No:-2456-2165 https://doi.org/10.38124/ijisrt/26nov472

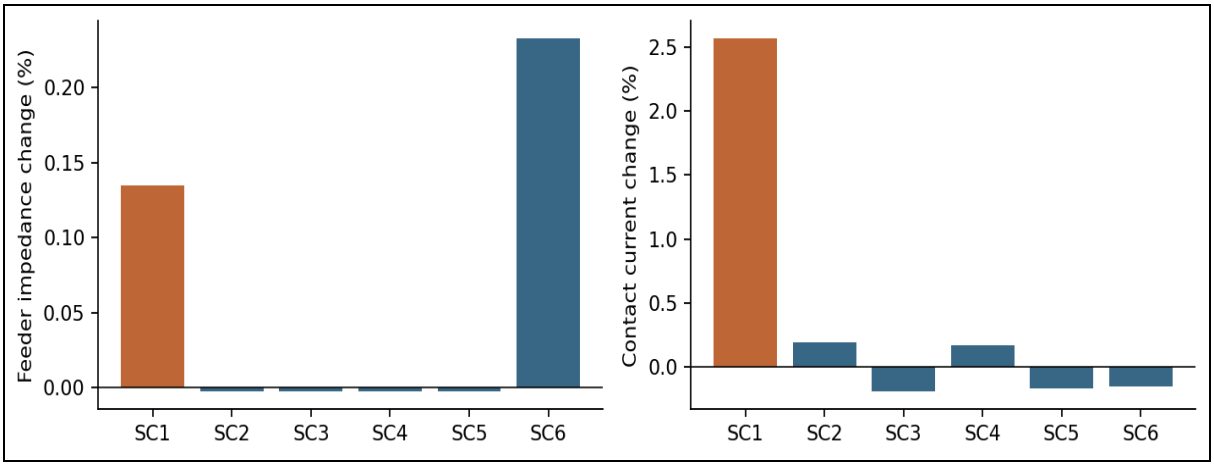


Fig 3 Changes in Line Impedance and Contact Current Relative to SC0. SC1 Also Changes Electrode Resistanc

➢ *Time-Domain Response and Fault Position*

Before the contract is applied, the scenarios have similar normal currents. After 0.2 s, the low-resistance contacts produced a large increase in source current and a collapse of receiving voltage. The downstream current becomes very small, approximately 0.012 A. SC1R retains an appreciable downstream current because its contact resistance is higher. The post-contact waveforms remain periodic at 50 Hz.

- *SC0 Homogeneous Reference Soil*

Fig. 4a shows the time-domain response of the SWER feeder before and after contact under homogeneous soil conditions. This scenario serves as the reference for the other cases.

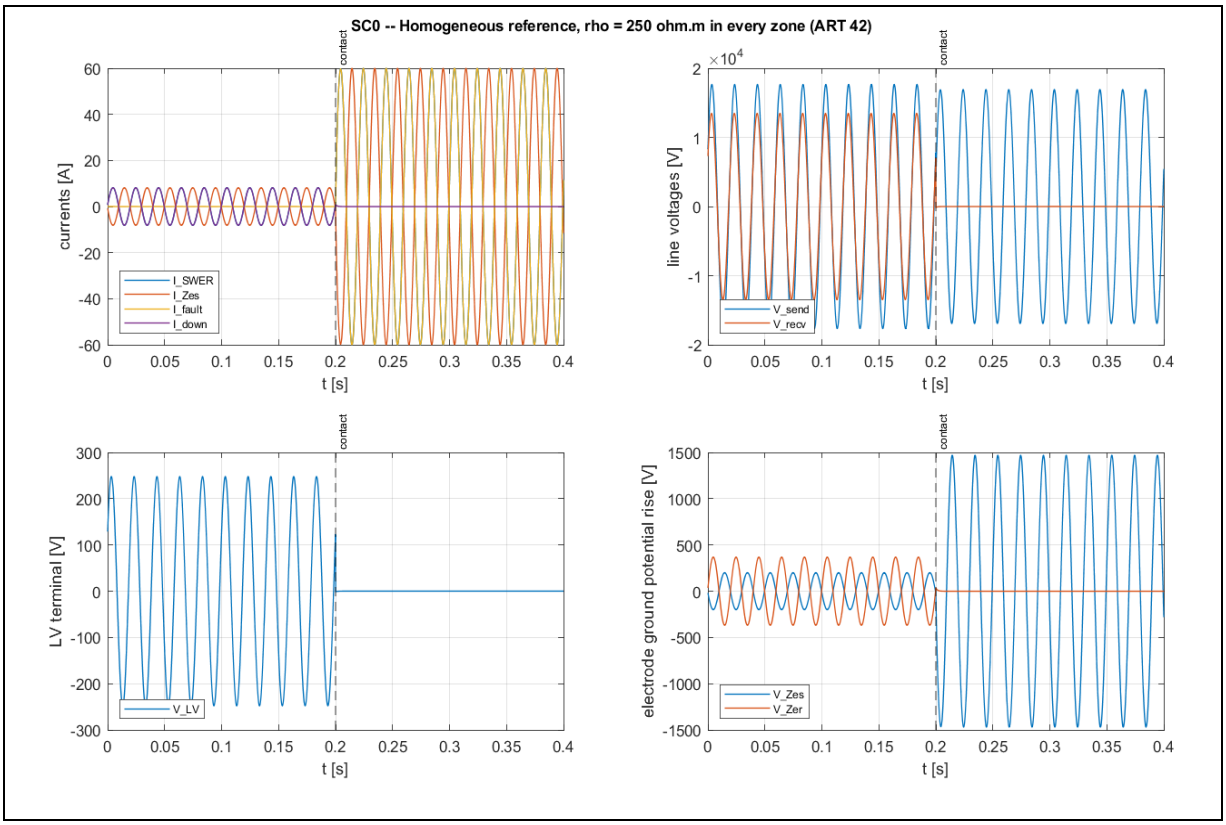


Fig 4a Time-Domain Response of SC0. Contact Applied at 0.2 s, 44 km from the Source on 80 km Feeder.

SC0 establishes the reference response. Normal current is 5.774 A. After the contact, contact current reaches 42.383 A and downstream current falls to approximately 0.012 A.

- *SC1 Combined Longitudinal and Vertical Heterogeneity*

Fig 4b shows the feeder response when soil resistivity varies both along the route and with depth. Electrode resistance also differs from those in SC0.

ISSN No:-2456-2165 https://doi.org/10.38124/ijisrt/26nov472

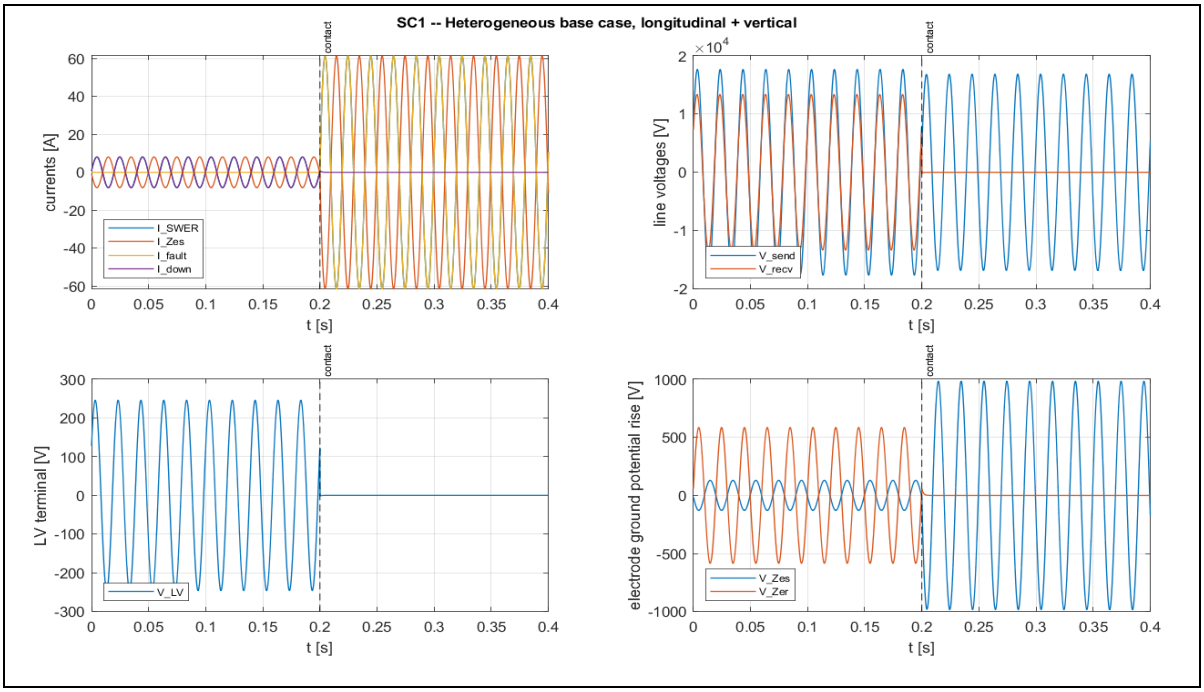


Fig 4b Time-Domain Response of SC1. Contact Applied at 0.2 s, 44 km from the Source on the 80 km Feeder.

Normal current is 5.726 A, and contact current reaches 43.471 A. Receiving voltage collapses after the contact. The comparison with SC0 includes changes in both soil impedance and electrode resistance.

- *SC1R Heterogeneous Soil with a 500 Ω Contact*

Fig. 4c shows how increasing the contact resistance to 500 Ω in the SC1 soil configuration affects the contact current and the electrical response downstream of the contact point.

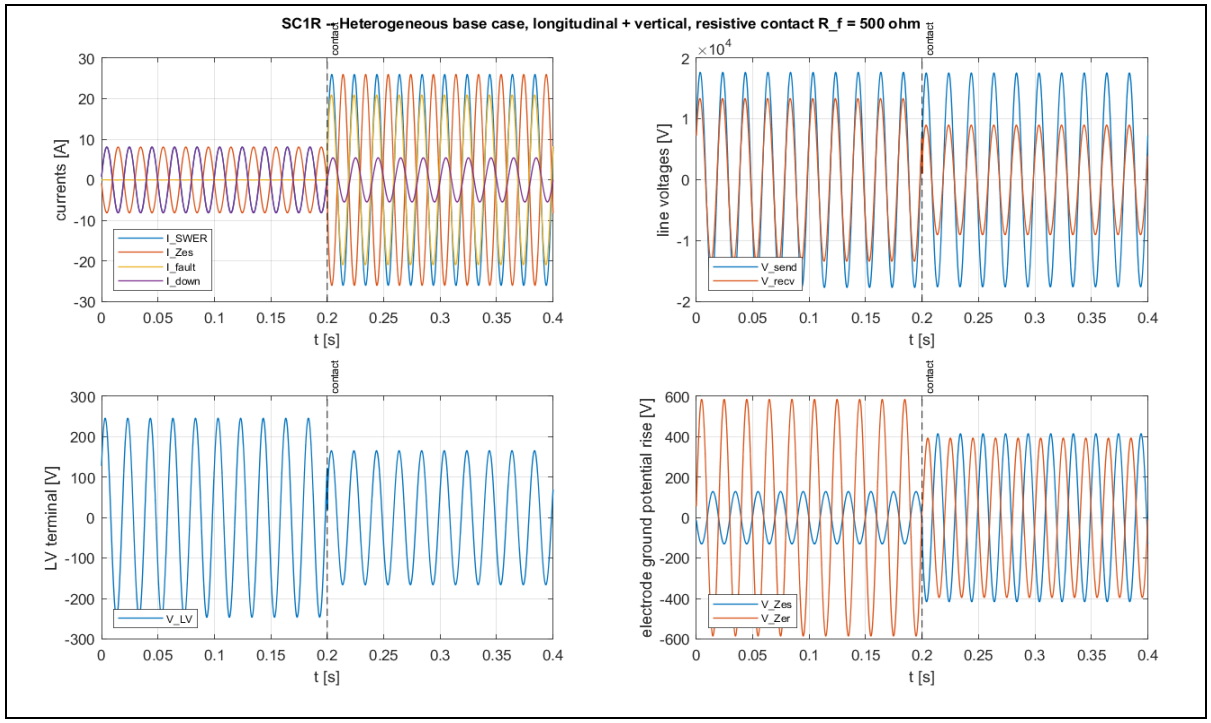


Fig 4c. Time-Domain Response of SC1R. Contact Applied at 0.2 s, 44 km from the Source on the 80 km Feeder.

The contact limits contact current to 14.778 A. A downstream current of 3.851 A remains, and the receiving voltage does not collapse as it does for the low-resistance contacts.

- *SC2 Abrupt Resistivity Changes from 50 to 1250 Ω·m*

Fig4d shows the feeder response when soil resistivity changes abruptly between zones, with values ranging from 50 to 1,250 Ω·m.

ISSN No:-2456-2165 https://doi.org/10.38124/ijisrt/26nov472

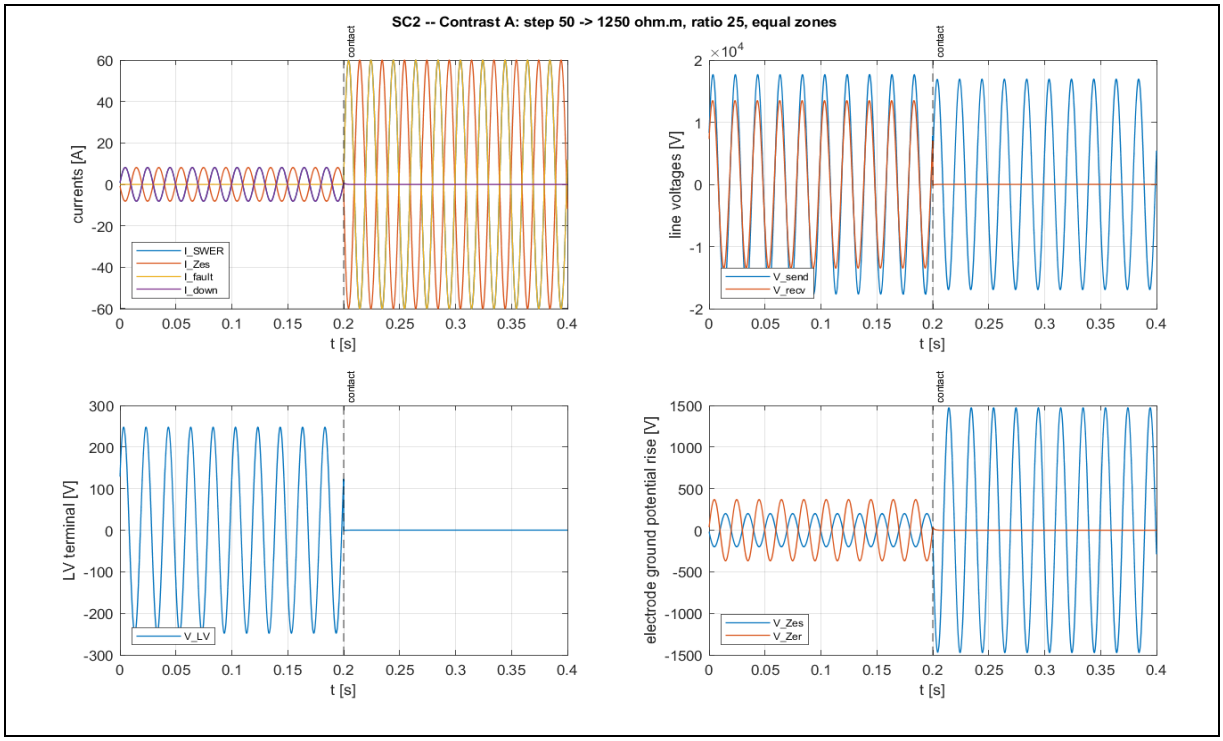


Fig 4d. Time-Domain Response of SC2. Contact Applied at 0.2 s, 44 km from the Source on the 80 km Feeder.

Normal current is 5.774 A and contact current reaches 42.465 A. Its response is close to SC0 because electrode resistances are fixed and line impedance changes only slightly distributed.

- *SC3 Reversed Zone Order of SC2*

Fig. 4e In SC3, the soil zones defined in SC2 are arranged in reverse order Comparing the two scenarios illustrates how the position of the zones relative to the contact point affects the contact current.

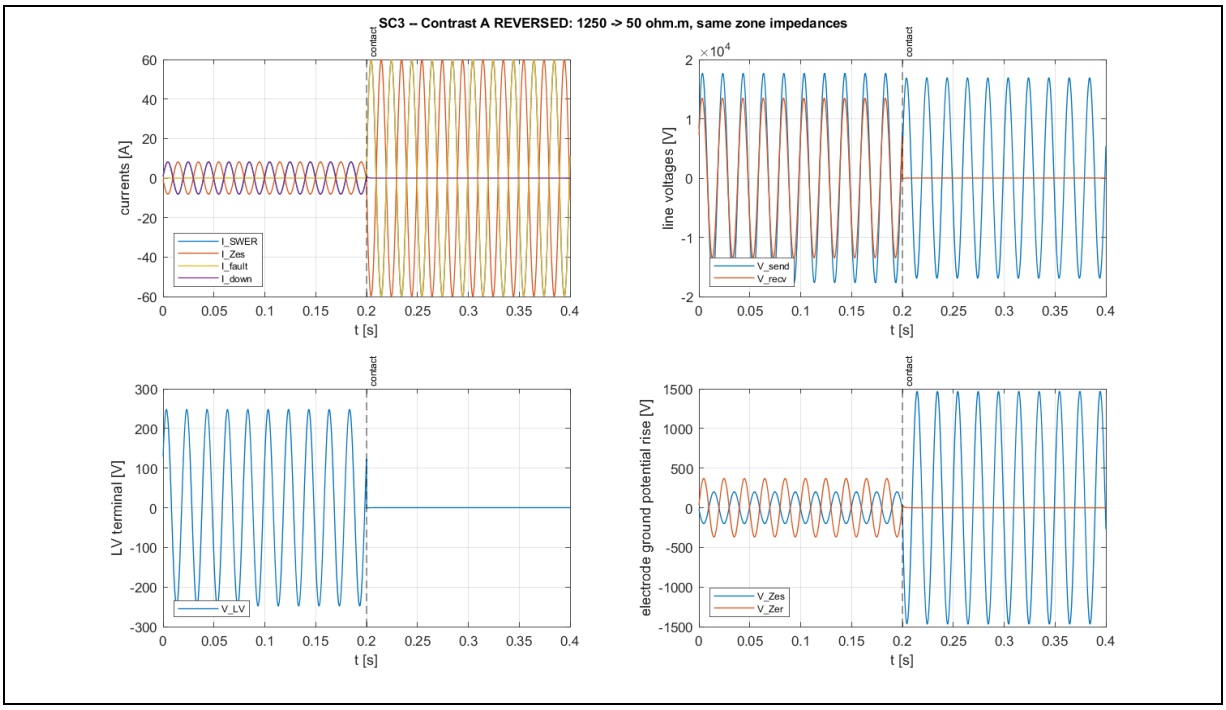


Fig 4e. Time-Domain Response of SC3. Contact Applied at 0.2 s, 44 km from the Source on the 80 km Feeder.

Contact current reaches 42.300 A, slightly below SC2. Reversing the zones changes upstream impedance at the contact while preserving total line impedance.

- *SC4 Progressive Resistivity Variation from 25 to 2500 Ω·m*

To examine the response to a gradual change in soil resistivity, SC4 uses a profile that increases from 25 to 2,500 Ω·m along the feeder at Fig. 4f**.**

ISSN No:-2456-2165 https://doi.org/10.38124/ijisrt/26nov472

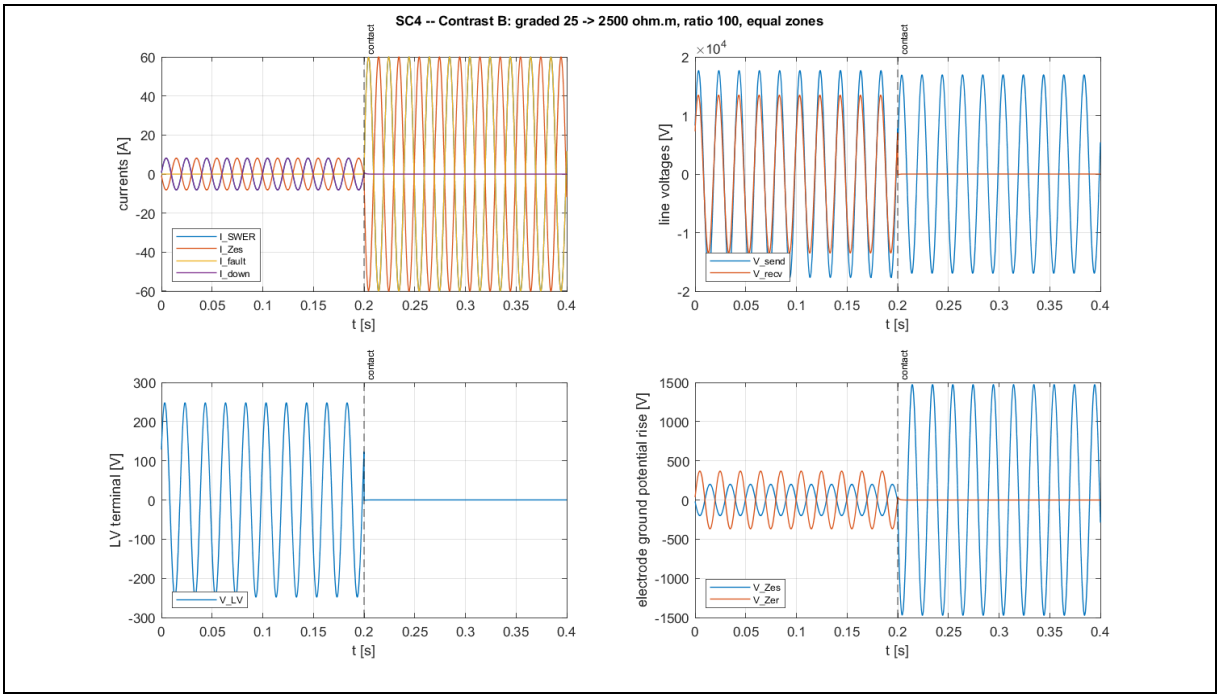


Fig 4f. Time-Domain Response of SC4. Contact Applied at 0.2 s, 44 km from the Source on the 80 km Feeder.

Contact current reaches 42.454 A. The waveforms remain close to those of the homogeneous reference, with a very small downstream current after the contact.

- *SC5 Reversed Resistivity Gradient of SC4*

With the highest-resistivity zone closest to the source, SC5 reverses the gradient used in SC4. The resulting feeder response is presented in Fig. 4g.

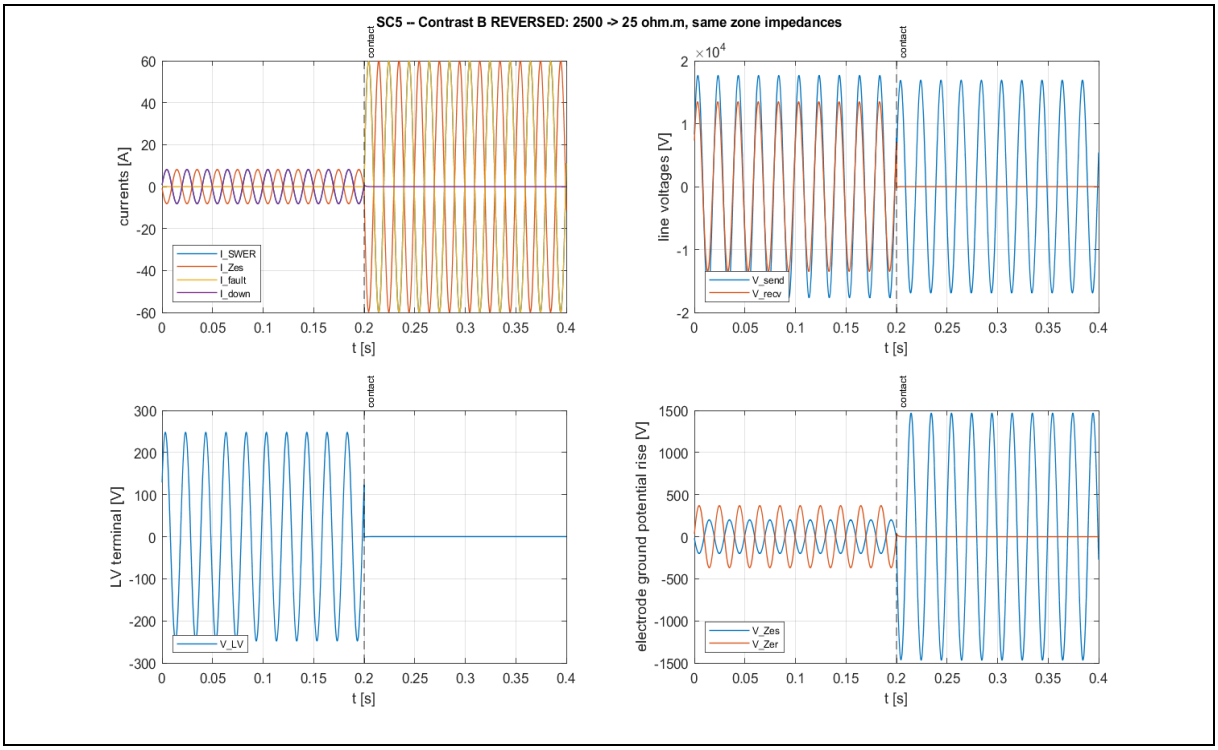


Fig 4g. Time-Domain Response of SC5. Contact Applied at 0.2 s, 44 km from the Source on the 80 km Feeder.

Contact current reaches 42.311 A. The small reduction compared with SC4 shows the effect of zone order on the upstream path to the contact.

- *SC6 Vertical Stratification in Every Zone*

Vertical soil stratification is included in every zone of SC6 Fig. 4). To assess its effect on the feeder response, electrode resistances are held at their reference values.

ISSN No:-2456-2165 https://doi.org/10.38124/ijisrt/26nov472

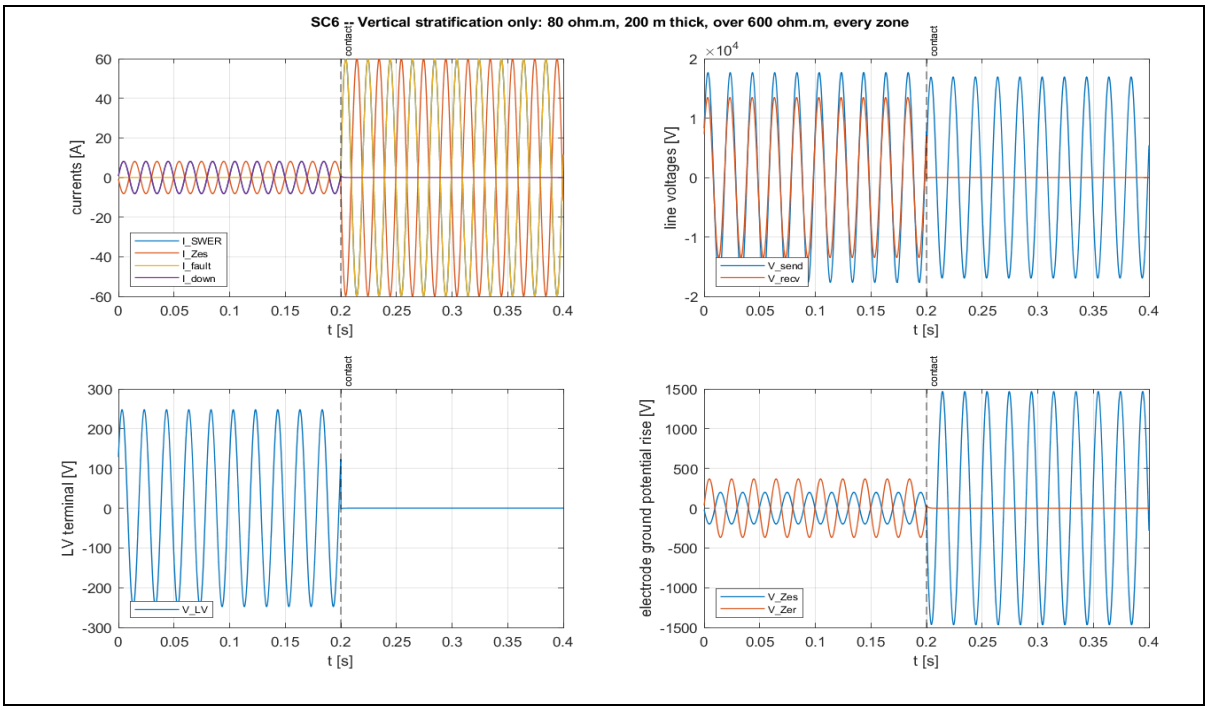


Fig 4h. Time-Domain Response of SC6. Contact Applied at 0.2 s, 44 km from the Source on the 80 km Feeder.

Normal current is 5.772 A and contact current reaches 42.318 A. With electrode resistances fixed, this vertical soil profile produces only small current changes relative to SC0.

The fault-position sweep shows that contact current decreases as the contact moves away from the source. More distant contact includes a larger upstream line impedance. SC1R has a lower contact current than the low-resistance cases. SC2–SC6 produce closely spaced curves, consistent with their small differences in distributed line impedance.

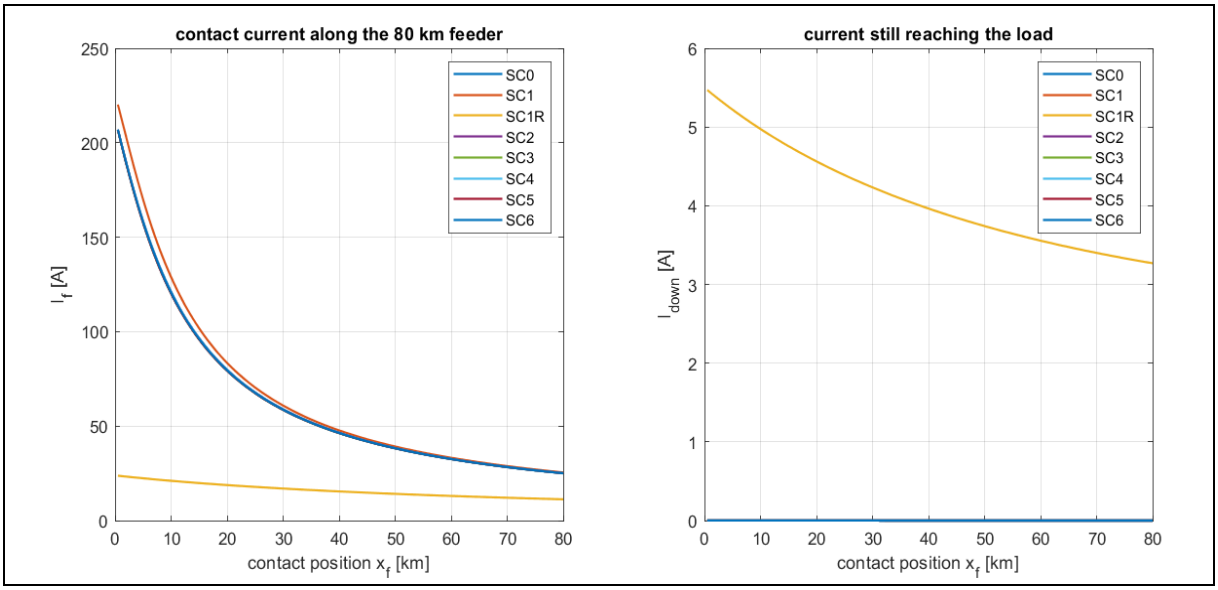


Fig 5 Contact Current and Downstream Current Versus Contact Position for the Simulated Scenarios.

➢ *Effect of Reversing the Zone Order*

Reversing SC2 to SC3 leaves the total line impedance unchanged but increases the magnitude of the upstream impedance at the contact by 0.217 per cent. The contact current decreases from 42.465 to 42.300 A, a reduction of 0.389 %. Reversing SC4 to SC5 increases the upstream impedance by 0.188 per cent and reduces the contact current from 42.454 to 42.311 A, a reduction of 0.337 %.

These differences are small but not zero. In the series-zone model, the same zone impedances give the same total when their order is changed. However, internal contact depends on the zones located between the source and the contact. The position of the zones therefore has a measurable, albeit small, effect on the contact current [13] [14].

➢ *Vertical Stratification and Sensitivity*

In the SC6 configuration, a layer with a resistivity of 80 Ω·m and a thickness of 200 m covers half-space with a

ISSN No:-2456-2165 https://doi.org/10.38124/ijisrt/26nov472

resistivity of 600 Ω·m in each zone. The electrode resistance remains fixed at the values for the SC0 configuration. The line impedance increases by 0.233 %, whilst the normal current decreases by 0.031 per cent and the contact current decreases by 0.154 per cent. The changes in current are therefore small for this configuration. Configurations SC6 and SC0 exhibit different resistivity profiles; this comparison therefore does not allow the stratification with an identical average resistivity to be isolated.

Scanning the resistivity in uniform soil allows line effects and electrode effects to be distinguished. When the resistivity changes from 10 to 10,000 Ω·m and the electrodes follow the ground, the source electrode resistance increases from 0.98 to 980.37 Ω and the analytical contact current decreases from 46.53 to 10.22 A. Over the same range, the magnitude of the line impedance increases by only 0.583 %. With fixed electrode resistances, the analytical contact current decreases only from 43.00 to 42.57 A. In this test, the greatest variation in current is primarily attributable to the electrodes.

The SC1 sensitivity chain shows the same trend. A 10 per cent increase in the resistivity of the layer alters the real part of the equivalent resistivity by approximately 10.09 to 12.16 per cent and the absolute value of the complex depth by 4.88 to 5.86 per cent. However, the absolute value of the loop impedance varies by only 0.0056 to 0.0081 per cent. The distributed impedance therefore attenuates the disturbance to the soil resistivity.

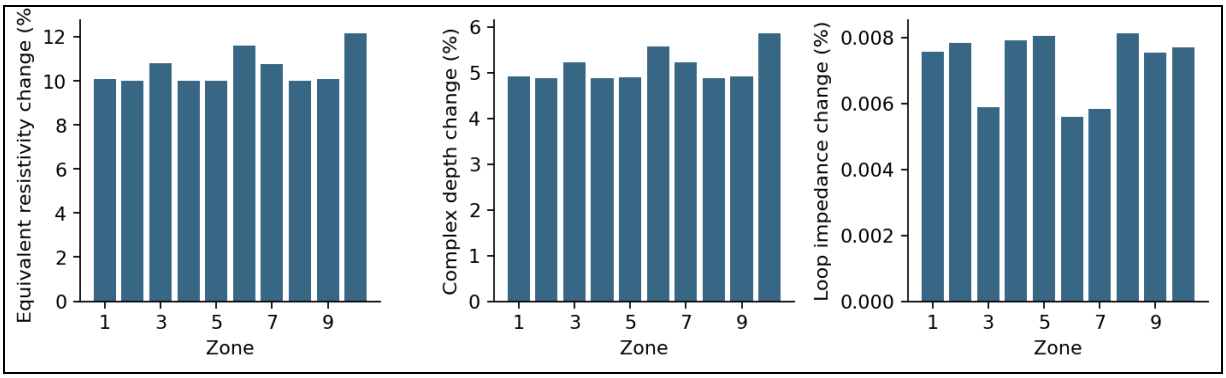


Fig 6 Sensitivity of the Equivalent Resistivity, Complex Depth and Loop Impedance to Variations in the Resistivity of the Layers in SC1.

The results of the discretization should be interpreted with caution. Between ten and forty zones, the line impedance varies by approximately 0.0032 % and the contact current by 0.0124 %, but the normal current varies by 1.61 % and the receiving GPR by approximately 45.2 %. The resistance of the receiving electrode is not kept constant in this comparison. This data therefore does not allow the convergence of all parameters to be established.

➢ *Circuit Topology Check*

The separate topology test confirms that Zag must represent a mutual coupling. For the SC0 parameter set used in this test, treating Zag as a branch to earth causes 99.48 % of the source current to bypass the load and reduces the voltage across the low-voltage terminals to 8.64 V. With the coupling representation, the source and load currents are equal, and the terminal voltage is 181.80 V. This is a verification of the circuit topology, distinct from the time-domain scenario results presented in Table 2.

➢ *Discussion and Limitations*

For this 50 Hz power line, the soil configurations tested have a minor impact on the line's total impedance. Variations in the local resistance of the electrodes result in more significant variations in the ground potential rise and contact current. Reversing the order of the zones also affects an internal fault, even when the line's total impedance remains unchanged.

The model represents the line as a set of concentrated zones. It does not consider three-dimensional soil interfaces, local contact and step voltages, arcing or soil ionization. The profiles constitute simulation scenarios rather than measurements taken along a specific route under study. The results describe the power line under study and should not be directly generalized to other geometries or to fast transients. Experimental validation would require measured soil profiles, electrode resistances, voltages and currents.

IV. CONCLUSION

In this article, we have developed a SWER line model capable of handling heterogeneous soils by combining several key elements: vertical homogenization of the soil, division of the line into successive zones, classical primitive impedance matrices, explicit modelling of earthing electrodes, and the ability to move the conductor-to-earth fault point along the line. What makes this approach useful is that it establishes a coherent link between electromagnetic return calculations and their practical implementation in Simulink, without sacrificing the mutual coupling between conductors.

For the 80 km power line studied at 50 Hz, the ground configurations tested result in minor variations in the line's total impedance. More significant variations in contact current and ground potential rise occur when the electrode resistances also vary. Reversing the order of the zones preserves the total line impedance but reduces the contact current at km 44 by approximately 0.39 % for SC2–SC3 and by 0.34 % for SC4–SC5. Deri's formulation remains close to that of Carson, with an average relative error on the

ISSN No:-2456-2165 https://doi.org/10.38124/ijisrt/26nov472

complex impedance of approximately 0.08 %. The discrepancies between the simulated and analytical currents remain below approximately 1 %, which confirms the numerical validity of the circuit implementation. However, the discretization study does not establish convergence for all quantities, as the resistance of the receiving electrode varies between the cases compared.

The modelling approach developed in this study and the results obtained provide a foundation for analyzing the electrical behavior of SWER lines in heterogeneous soils. Future work can build on these findings by using measurements from an operating SWER line to validate the model and extend the analysis.

REFERENCES

[1]. N. Hosseinzadeh, J. E. Mayer, and P. J. Wolfs, "Rural single wire earth returns distribution networks: Associated problems and cost-effective solutions," Int. J. Electr. Power Energy Syst., vol. 33, 2011.
[2]. A. C. Britten, "Single-wire earth return systems in Eskom," in Proc. African Utility Week, South Africa.
[3]. M. A. Kashem and G. Ledwich, "Distributed generation as voltage support for single wire earth return systems," IEEE Trans. Power Deliv., vol. 19, no. 3, pp. 1002–1011, Jul. 2004, doi: 10.1109/TPWRD.2003.822977.
[4]. G. Bakkabulindi, M. R. Hesamzadeh, M. Amelin, and I. N. Da Silva, "Models for conductor size selection in single wire earth return distribution networks," IEEE Trans. Power Deliv., 2013.
[5]. J. R. Carson, "Wave propagation in overhead wires with ground return," Bell Syst. Tech. J., vol. 5, no. 4, pp. 539–554, 1926.
[6]. A. Deri, G. Tevan, A. Semlyen, and A. Castanheira, "The complex ground return plane: A simplified model for homogeneous and multi-layer earth return," IEEE Trans. Power App. Syst., vol. PAS-100, no. 8, pp. 3686–3693, 1981.
[7]. M. Nakagawa, A. Ametani, and K. Iwamoto, "Further studies on wave propagation in overhead lines with earth return: Impedance of stratified earth," Proc. Inst. Electr. Eng., vol. 120, 1973.
[8]. T. Noda, "A double logarithmic approximation of Carson's ground-return impedance," IEEE Trans. Power Deliv., vol. 21, no. 1, pp. 472–479, Jan. 2006.
[9]. I. Kim, "A new single-logarithmic approximation of Carson's ground-return impedances—Part 1," IEEE Access, vol. 9, 2021, doi: 10.1109/ACCESS.2021.3097377.
[10]. A. G. Martins-Britto, F. V. Lopes, and S. R. M. J. Rondineau, "Multi-layer earth structure approximation by a homogeneous conductivity soil for ground return impedance calculations," IEEE Trans. Power Deliv., 2020, doi: 10.1109/TPWRD.2019.2930406.
[11]. B. Nkom, A. P. R. Taylor, and C. Baguley, "Narrowband modeling of single-wire earth return distribution lines," IEEE Trans. Power Deliv., vol. 33, no. 4, pp. 1565–1575, Aug. 2018.
[12]. H. B. Dwight, "Calculation of resistances to ground," Electr. Eng., vol. 55, no. 12, pp. 1319–1328, 1936.
[13]. A. Semlyen and A. Deri, "Time domain modelling of frequency dependent three-phase transmission line impedance," IEEE Trans. Power App. Syst., vol. PAS-104, 1985.
[14]. A. Ametani, N. Nagaoka, Y. Baba, and T. Ohno, Power System Transients: Theory and Applications. Boca Raton, FL, USA: CRC Press, 2014.
[15]. IEEE Guide for Safety in AC Substation Grounding, IEEE Std 80-2013, 2013.
[16]. A. Ametani, N. Nagaoka, Y. Baba, and T. Ohno, Power System Transients: Theory and Applications. Boca Raton, FL, USA: CRC Press, 2014.